

High-redshift JWST massive galaxies and the initial clustering of supermassive primordial black holes

HAI-LONG HUANG ^{1,2} JUN-QIAN JIANG ² AND YUN-SONG PIAO^{1,2,3,4}

¹*School of Fundamental Physics and Mathematical Sciences, Hangzhou Institute for Advanced Study, UCAS, Hangzhou 310024, China*

²*School of Physical Sciences, University of Chinese Academy of Sciences, Beijing 100049, China*

³*International Center for Theoretical Physics Asia-Pacific, Beijing/Hangzhou, China*

⁴*Institute of Theoretical Physics, Chinese Academy of Sciences, P.O. Box 2735, Beijing 100190, China*

ABSTRACT

In this paper, we show that the initial clustering of supermassive primordial black holes (SMPBHs) beyond a Poisson distribution can efficiently enhance the matter power spectrum, and thus the halo mass function. As a result, the population of initially clustered SMPBHs with $M_{\text{PBH}} \sim 10^9 M_{\odot}$ and the fraction of energy density $f_{\text{PBH}} \sim 10^{-3}$ (consistent with current constraints on SMPBHs) has the potential to naturally explain high-redshift massive galaxies observed by the James Webb Space Telescope.

Keywords: Early universe — Galaxy formation — Supermassive black holes

1. INTRODUCTION

Recent observations with the James Webb Space Telescope (JWST) have discovered a large number of quasars powered by supermassive black holes (SMBHs) already in place within the first few hundred million years after the Big Bang (e.g. Harikane et al. 2023; Larson et al. 2023; Maiolino et al. 2023a; Matthee et al. 2023; Übler et al. 2023a; Goulding et al. 2023; Kokorev et al. 2023; Übler et al. 2023b; Furtak et al. 2023; Maiolino et al. 2023b; Bogdán et al. 2024; Greene et al. 2024; Nataraajan et al. 2024; Kovács et al. 2024). The existence of such SMBHs at very high redshifts poses a significant challenge. It is commonly assumed that SMBH seeds initially form, such as seed black holes expected from Pop III stellar remnants (Madau & Rees 2001), and then grow into SMBHs over time until the redshifts of observations. However, even if they accrete at the maximal Eddington rate, there does not seem to be enough cos-

mic time to grow them sufficiently.¹ In this scenario, the direct birth of SMBHs in the very early Universe, i.e., SMPBHs, becomes rather appealing.

The initial clustering of stellar-mass PBHs has been ruled out by microlensing and Lyman- α forest observations (De Luca et al. 2022). However, it seems that SMPBHs prefer an initially clustered spatial distribution. In the standard mechanism that PBHs are from a direct collapse of large amplitude perturbations after horizon entry (e.g. Sasaki et al. 2018; Carr et al. 2021; Green & Kavanagh 2021; Escrivà et al. 2022; Green 2024), non-Gaussian primordial perturbations seems to necessary to evade the μ -distortion constraints for SMPBHs (Nakama et al. 2018; Ünal et al. 2021; Gow et al. 2023; Hooper et al. 2024; Byrnes et al. 2024; Sharma et al. 2024; Cai et al. 2024), while the non-Gaussianity of primordial perturbation will possibly lead to the initial clustering of SMPBHs (Franciolini et al. 2018; Tada & Yokoyama 2015; Young & Byrnes 2015; Suyama & Yokoyama 2019). In the mechanism (Huang et al. 2023; Huang & Piao 2023) where SMPBHs are

¹ It might be thought the hypothesis that heavy seeds could be direct collapse black holes (DCBHs) might alleviate this problem. However, DCBHs have long been considered too rare to account for the entire observed SMBH population, see also Bhowmick et al. (2024) for recent numerical simulations.

sourced by the inflationary bubbles and have a multi-peak mass spectrum, the PBHs can be spatial-clustered naturally in multistream inflation (Li & Wang 2009; Li et al. 2009), see also Huang & Piao (2023); Ding et al. (2019); Li et al. (2021). The PBHs from Affleck-Dine mechanism also show a strong clustering (Kawasaki et al. 2021; Kasai et al. 2024), see also Kasai et al. (2023).

It has been showed in Huang et al. (2023); Huang & Piao (2023); Gouttenoire et al. (2023); Depta et al. (2023); Huang et al. (2024) that the merger of SMPBHs might be the source of nano-Hertz gravitational wave background recently detected by pulsar timing arrays (PTA) collaborations (Agazie et al. 2023; Xu et al. 2023; Reardon et al. 2023; EPTA Collaboration et al. 2023), however, the distribution of SMPBHs must exhibit some clustering to magnify the merger rate of SMPBH binaries. On the other hand, considering the non-zero angular auto-correlation function of quasars (Efstathiou & Rees 1988; Cole & Kaiser 1989), models predicting the Poisson distribution of SMPBHs are ruled out. The Sloan Digital Sky Survey (York et al. 2000) and the 2dF QSO redshift survey (Croom et al. 2004) have measured the auto-correlation function of quasars up to $z \approx 4$ (e.g. Pizzati et al. 2024a,b). The auto-correlation function of faint quasars at $z \approx 6$ was also recently estimated, benefiting from the high sensitivity of the Subaru High- z Exploration of Low-Luminosity Quasars survey (Arita et al. 2023).

Recently, based on 14 galaxy candidates with masses in the range $10^9 - 10^{11} M_\odot$ at $7 < z < 11$ identified in the JWST Cosmic Evolution Early Release Science program, Labbé et al. (2023) found that the cumulative stellar mass density at redshift $z^{\text{obs}} = 8$ for the stellar mass density $M_* \geq 10^{10} M_\odot$ is

$$\rho^{\text{obs}}(M_* \geq 10^{10} M_\odot) \simeq 1.3 \times 10^6 M_\odot \text{Mpc}^{-3}. \quad (1)$$

This result is hardly reconcilable with the standard Λ Cold Dark Matter model (Λ CDM) expectation, which would require an implausible high star formation efficiency, even larger than the cosmic baryon mass budget in collapsed structures. This conflict has inspired lots of relevant studies (e.g. Biagetti et al. 2023; Hütsi et al. 2023; Jiao et al. 2023; Yuan et al. 2023; Parashari & Laha 2023; Padmanabhan & Loeb 2023; Adil et al. 2023; Davari et al. 2023; Forconi et al. 2024; Menci et al. 2024; Paraskevas et al. 2024; Iocco & Visinelli 2024a).

However, if SMPBHs do exist, they would enhance the halo mass function and thus boost the early formation of massive galaxies (e.g. Liu & Bromm 2022, 2023; Colazo et al. 2024; Zhang et al. 2024; Biagetti et al. 2023). In this paper, we explore the effect of the initial clustering of SMPBHs. It is found that the initial clustering can

further enhance the halo mass function at the high mass tail. As a result, the population of initially clustered SMPBHs with $M_{\text{PBH}} \sim 10^9 M_\odot$ and $f_{\text{PBH}} \sim 10^{-3}$ (consistent with current constraints on SMPBHs e.g. Carr et al. (2024)) has the potential to naturally explain high-redshift massive galaxies observed by JWST. The results are summarised in Fig. 1.

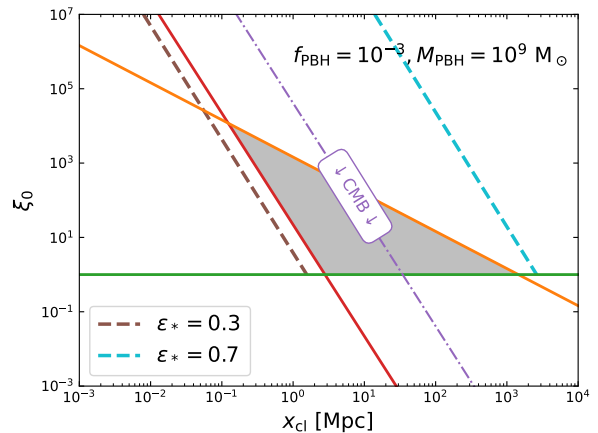


Figure 1. The parameter space of (ξ_0, x_{cl}) for initially clustered SMPBHs explaining the JWST observation, where we have assumed $M_{\text{PBH}} = 10^9 M_\odot$ and $f_{\text{PBH}} = 10^{-3}$. The gray shaded region represents the parameter space allowed by the model itself, constrained by Eq. (6) (green), Eq. (7) (red) and Eq. (8) (orange), respectively. The purple line represents the observation constraint from the CMB, Eq. (22). The brown (cyan) line indicate clustering SMPBH which can explain the comoving cumulative stellar mass density for the star formation rate $\epsilon_* = 0.3$ (0.7). We do not consider the enhancement of the PBH isocurvature power spectrum at $k > k_{\text{cut,cluster}}$ (see Eq. (19) and the discussion nearby), and any correlation between the adiabatic and isocurvature modes is ignored here. Therefore, the estimates of the required star formation efficiency shown here are the most conservative results in clustered SMPBH model.

2. MODELLING INITIAL CLUSTERING OF PBHS

The clustering of PBHs beyond the Poisson distribution is described by its correlation functions, and the precise shape is model-dependent. Here, for simplicity the correlation function of PBHs is modelled as (De Luca et al. 2022)

$$\xi_{\text{PBH}}(x) = \begin{cases} \xi_0 & \text{if } x \leq x_{\text{cl}}, \\ 0 & \text{otherwise,} \end{cases} \quad (2)$$

where x_{cl} is the comoving size of the gravitationally bound cluster. The corresponding PBH clusters follow a Poisson distribution at much large scales.

It has been argued in [Desjacques & Riotto \(2018\)](#) that PBHs are anti-correlated at short distances as one should expect that there is at most one PBH per horizon volume, i.e. $\xi_{\text{PBH}}(x) \simeq -1$ for $x \lesssim x_{\text{exc}}$, where the comoving size x_{exc} of the small-scale exclusion volume is approximately the comoving Hubble radius at formation time of PBHs,

$$x_{\text{exc}} \simeq x_H \simeq \left(\frac{M_{\text{PBH}}}{M_{\odot}} \right)^{1/2} \frac{1}{4 \times 10^6 \text{ Mpc}^{-1}}. \quad (3)$$

We have verified that the spatial exclusion condition has negligible effect on our subsequent calculations ($x_{\text{exc}} \ll x_{\text{cl}}$), allowing us to safely adopt Eq. (2).

Here, for analytical viability, we adopt a monochromatic PBH mass function with a mass parameter M_{PBH} and the fraction of dark matter (DM) $f_{\text{PBH}} = \Omega_{\text{PBH}}/\Omega_{\text{DM}}$. The average energy density of PBHs is $\bar{\rho}_{\text{PBH}} = \bar{n}_{\text{PBH}} M_{\text{PBH}}$, where the average (comoving) number density is

$$\bar{n}_{\text{PBH}} \simeq 3.3 \times 10^{10} f_{\text{PBH}} \left(\frac{M_{\text{PBH}}}{M_{\odot}} \right)^{-1} \text{ Mpc}^{-3}. \quad (4)$$

In such a PBH cluster, the number of PBHs is

$$N_{\text{cl}} = 1 + \bar{n}_{\text{PBH}} \int d^3x \xi_{\text{PBH}}(x), \quad (5)$$

see [De Luca et al. \(2022\)](#) for details, which is approximately $N_{\text{cl}} \simeq \frac{4\pi}{3} \bar{n}_{\text{PBH}} \xi_0 x_{\text{cl}}^3$. Thus we have that

$$\xi_0 \simeq \frac{N_{\text{cl}} / \frac{4}{3} \pi x_{\text{cl}}^3}{\bar{n}_{\text{PBH}}} \equiv \frac{\bar{n}_{\text{PBH,cl}}}{\bar{n}_{\text{PBH}}} > 1 \quad (6)$$

represents the ratio of the number density of PBHs within the cluster to the average number density approximately. The Poisson distribution corresponds to $\xi_{\text{PBH}}(x) = 0$, or equivalently, $N_{\text{cl}} = 1$.

In clustered scenarios, we should assume that $N_{\text{cl}} \gtrsim 3$, i.e.

$$\xi_0 \gtrsim 2.2 \times 10^{-11} f_{\text{PBH}}^{-1} \left(\frac{M_{\text{PBH}}}{M_{\odot}} \right) \left(\frac{x_{\text{cl}}}{\text{Mpc}} \right)^{-3}. \quad (7)$$

Additionally, it is required that the cluster does not collapse into a heavy PBH with mass of $N_{\text{cl}} M_{\text{PBH}}$, which suggests ([De Luca et al. 2022, 2023](#))

$$\xi_0 \lesssim 60 f_{\text{PBH}}^{-1/3} \left(\frac{C}{200} \right)^{-1/6} \left(\frac{x_{\text{cl}}}{\text{Mpc}} \right)^{-1} \quad (8)$$

according to the hoop condition $r_{\text{cl}} \lesssim 2GM_{\text{cl}}$, where $C = \mathcal{O}(1-100)$ is a constant of proportionality, r_{cl} and M_{cl} are the physical radius and mass of the cluster.

3. THOSE ENHANCED BY CLUSTERING SMPBHs

3.1. Power spectrum

The density fluctuation of PBHs is

$$\delta_{\text{PBH}}(\mathbf{x}) \equiv \frac{\delta_{\text{PBH}}(\mathbf{x})}{\bar{\rho}_{\text{PBH}}} = \frac{1}{\bar{n}_{\text{PBH}}} \sum_i \delta_D(\mathbf{x} - \mathbf{x}_i) - 1, \quad (9)$$

noting that these PBHs are spatially discrete objects. $\delta_D(\mathbf{x})$ is the three-dimensional Dirac distribution. The corresponding two-point correlation function of fluctuation is given by

$$\langle \delta_{\text{PBH}}(0) \delta_{\text{PBH}}(\mathbf{x}) \rangle = \frac{1}{\bar{n}_{\text{PBH}}} \delta_D(\mathbf{x}) + \xi_{\text{PBH}}(x), \quad (10)$$

where $x = |\mathbf{x}|$ is the distance between two PBHs.

The power spectrum of the density perturbations of PBHs is

$$\begin{aligned} P_{\text{PBH}}(k) &= \int d^3\mathbf{x} e^{-i\mathbf{k}\cdot\mathbf{x}} \langle \delta_{\text{PBH}}(0) \delta_{\text{PBH}}(\mathbf{x}) \rangle \\ &= P_{\text{Poisson}}(k) + P_{\xi}(k), \end{aligned} \quad (11)$$

where $P_{\text{Poisson}}(k) = 1/\bar{n}_{\text{PBH}}$, which is independent of k , comes from the Poisson fluctuation induced by the fluctuation of the number of PBHs, and

$$P_{\xi}(k) = \int d^3\mathbf{x} e^{-i\mathbf{k}\cdot\mathbf{x}} \xi_{\text{PBH}}(x) = 4\pi \int dx x^2 \frac{\sin kx}{kx} \xi_{\text{PBH}}(x) \quad (12)$$

comes from the clustered distribution of PBHs. Thus considering Eq. (2), we have

$$P_{\xi}(k) = \frac{4\pi \xi_0 [\sin(kx_{\text{cl}}) - kx_{\text{cl}} \cos(kx_{\text{cl}})]}{k^3}. \quad (13)$$

We observe that

$$\lim_{k \rightarrow 0} P_{\xi}(k) = \frac{4\pi}{3} x_{\text{cl}}^3 \xi_0 \simeq \frac{N_{\text{cl}}}{\bar{n}_{\text{PBH}}} > \frac{1}{\bar{n}_{\text{PBH}}} = P_{\text{Poisson}}, \quad (14)$$

which indicates that the contribution of clustering for the power spectrum $P_{\xi}(k)$ exceeds that of the Poisson fluctuation on large scales.

The PBHs contribute to the isocurvature perturbations through $f_{\text{PBH}}^2 P_{\text{PBH}}(k)$. These isocurvature fluctuations then grow during the matter-dominated era, and at $z = 0$, they are given by

$$P_{\text{iso}}(k, z = 0) = \begin{cases} [f_{\text{PBH}} D_{\text{PBH}}(0)]^2 P_{\text{PBH}}(k), & \text{if } k \leq k_{\text{cut}}, \\ 0, & \text{otherwise,} \end{cases} \quad (15)$$

where $D_{\text{PBH}}(z) \simeq \left(1 + \frac{3\gamma}{2\alpha_-} \frac{1+z_{\text{eq}}}{1+z} \right)^{a_-}$ with $\gamma = (\Omega_m - \Omega_b)/\Omega_m$ and $a_- = (\sqrt{1+24\gamma} - 1)/4$ is the growth factor of isocurvature perturbations until today ([Inman](#)

& Ali-Haïmoud 2019; Gouttenoire et al. 2023). These isocurvature fluctuations are restricted to large scales, because we expect the linear theory to break down at small scales. For initially Poisson-distributed PBHs, the cut-off scale of the spectrum is of order the inverse mean separation between PBHs ²

$$k_{\text{cut,Poisson}} = (2\pi^2 \bar{n}_{\text{PBH}})^{1/3}. \quad (16)$$

At scales below $k_{\text{cut,Poisson}}$, we will have a single PBH within the corresponding comoving sphere, signaling the onset of the seed effect prevailing over the Poisson effect (Inman & Ali-Haïmoud 2019; Hütsi et al. 2023; Carr & Silk 2018). In the presence of initially clustering, we should replace it with the inverse average separation of clusters ³

$$k_{\text{cut,cluster}} = (2\pi^2 \bar{n}_{\text{cl}})^{1/3}, \quad (18)$$

where $\bar{n}_{\text{cl}} = \bar{n}_{\text{PBH}}/N_{\text{cl}}$ is the cluster number density. It is obvious that it corresponds to Eq. (16) when $N_{\text{cl}} = 1$ is satisfied, indicating the self-consistency of our model. Rewriting it with the model parameters (x_{cl}, ξ_0) , we have

$$k_{\text{cut,cluster}} \simeq \left(\frac{3\pi}{2\xi_0}\right)^{1/3} \frac{1}{x_{\text{cl}}}. \quad (19)$$

The Planck results (Planck Collaboration et al. 2020) set the upper bound on the primordial isocurvature perturbations on the CMB scale as

$$\beta_{\text{iso}}(k_{\text{CMB}}) \equiv \frac{P_{\text{iso}}(k_{\text{CMB}})}{P_{\text{iso}}(k_{\text{CMB}}) + P_{\mathcal{R}}(k_{\text{CMB}})}, \quad (20)$$

where $P_{\mathcal{R}}(k) = (2\pi^2/k^3)\mathcal{P}_{\mathcal{R}}$ with the power spectrum of curvature perturbations $\mathcal{P}_{\mathcal{R}}$. We conservatively use the constraint in Kawasaki et al. (2021), i.e. $\beta_{\text{iso}} < 0.035$ at $k_{\text{CMB}} = 2 \times 10^{-3} \text{ Mpc}^{-1}$. On such a large scale, the isocurvature perturbation Eq. (15) can be approximated as

$$P_{\text{iso}}(k) \simeq f_{\text{PBH}}^2 \times \frac{4\pi}{3} x_{\text{cl}}^3 \xi_0, \quad (21)$$

² Sometimes, a different choice of cut-off scale $k_{\text{NL}} \simeq (\bar{n}_{\text{PBH}}/f_{\text{PBH}})^{1/3}$ is adopted (e.g. Liu & Bromm 2022; Gouttenoire et al. 2023), below which the non-linear effects start to dominate. However, for the SMPBHs with $f_{\text{PBH}} \lesssim 10^{-3}$, our choice, Eq. (16), is more conservative. Additionally, the focus of our investigation is on the effect of the cluster distribution of PBHs compared to the Poisson distribution, so in the comparison we only need to maintain the same cut-off criteria.

³ We observe that

$$\bar{n}_{\text{cl}} = \frac{\bar{n}_{\text{PBH}}}{N_{\text{cl}}} < \bar{n}_{\text{PBH}} \xi_0 \simeq \bar{n}_{\text{PBH,cl}}, \quad (17)$$

ensuring that $\bar{n}_{\text{cl}}^{1/3} < \bar{n}_{\text{PBH,cl}}^{1/3}$, implying that the average separation between clusters (the minimal distance between PBHs located in different clusters) is bigger than that between individual PBHs within a cluster.

which suggests

$$\xi_0 < 4.1 \times 10^{-2} f_{\text{PBH}}^{-2} \left(\frac{x_{\text{cl}}}{\text{Mpc}}\right)^{-3}. \quad (22)$$

3.2. Halo mass function according to the power spectrum

We utilize the Sheth-Tormen (Sheth & Tormen 1999; Sheth et al. 2001) modification to the Press-Schechter formalism (Press & Schechter 1974) with a top-hat window function to calculate the halo mass function. The variance of the smoothed density is

$$\begin{aligned} \sigma^2(M) &= \int P_{\text{tot}}(k, z=0) W^2(kR) \frac{k^2 dk}{2\pi^2} \\ &= \int [P_{\Lambda\text{CDM}}(k, z=0) + P_{\text{iso}}(k, z=0)] W^2(kR) \frac{k^2 dk}{2\pi^2}, \end{aligned} \quad (23)$$

where $W(kR) = \frac{3[\sin(kR) - kR \cos(kR)]}{(kR)^3}$ is the window function, $R = \left(\frac{3M}{4\pi\rho_m}\right)^{1/3}$ is the comoving radius associated with the mass window M , and $P_{\Lambda\text{CDM}}(k)$ is the power spectrum of adiabatic perturbations for the ΛCDM model without SMPBHs.

The peak significance is defined as

$$\nu_c(M) = \frac{\delta_c}{\sigma(M, z)} = \frac{\delta_c}{D(z)\sigma(M)}, \quad (24)$$

where $D(z) \propto H(z) \int_z^{+\infty} dz' \frac{1+z'}{[H(z')]^3}$ is the linear growth function, normalized so that $D(0) = 1$. Here, we adopt $D(z) \approx 1.27/(1+z)$, which provides a good approximation at $z \gtrsim 1$ (Iocco & Visinelli 2024b). The comoving mean number density of halos $n_h(M)$ per logarithmic mass interval is

$$\frac{dn_h}{d \ln M_h} = \frac{\rho_m}{M_h} \nu_c(M_h) f(\nu_c(M_h)) \frac{d \ln \nu_c(M_h)}{d \ln M_h}, \quad (25)$$

where

$$\nu_c f(\nu_c) = \sqrt{\frac{2}{\pi}} A(p) \left[1 + \frac{1}{(q\nu_c^2)^p}\right] \sqrt{q\nu_c} e^{-q\nu_c^2/2} \quad (26)$$

with $A(p) = [1 + \pi^{-1/2} 2^{-p} \Gamma(0.5 - p)]^{-1}$. Here, we adopt $(q, p) = (0.85, 0.3)$, which has been found to provide an accurate fit to the N-body simulations at high redshifts (Schneider et al. 2021).

In Fig. 2, we depict the power spectrum and the corresponding halo mass function. The effect of SMPBHs is creating a small bulge in the matter power spectrum, with the position and height of the bulge depending on their number density, while for initial clustering SMPBHs, the bulge shifts to the left and its height slightly rises. As a result, the halo mass function is enhanced for $M_h > 10^{11} h^{-1} M_{\odot}$.

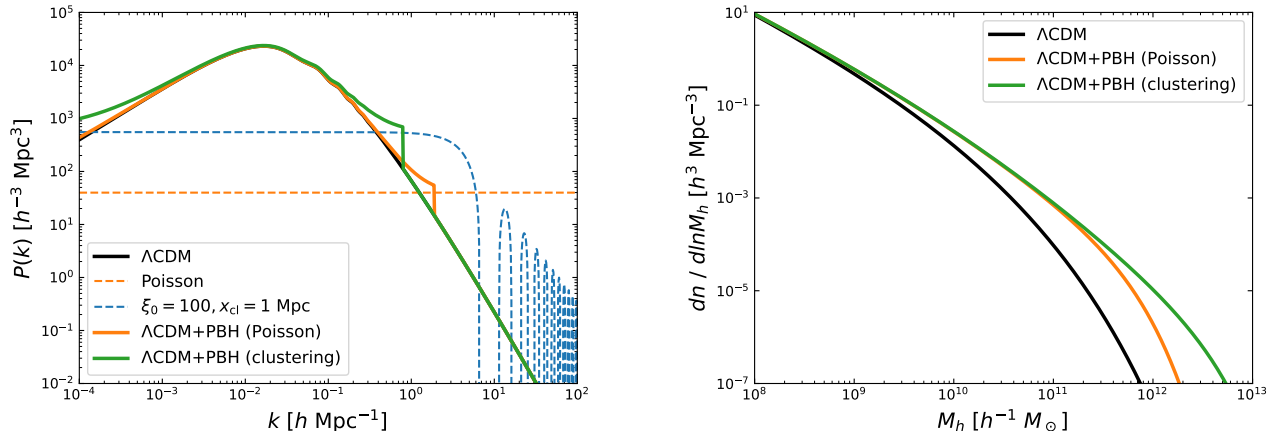


Figure 2. *Left panel:* The linear matter power spectrum at $z = 0$ is plotted for Λ CDM (black solid), for Λ CDM with initially Poisson-distributed SMPBHs ($\xi_{\text{PBH}}(x) = 0$, orange solid) and initially clustering SMPBHs (green solid), respectively, where $M_{\text{PBH}} = 10^9 M_{\odot}$ and $f_{\text{PBH}} = 10^{-3}$. The cut-off Eq. (16) and Eq. (19) are considered respectively. We also plot the isocurvature fluctuation sourced by the Poisson fluctuation (orange dashed) and clustered distribution (blue dashed). *Right panel:* The corresponding halo mass function at redshift $z = 8$.

4. EXPLAIN JWST OBSERVATIONS

In the following, we explore whether initially clustering SMPBH can explain the massive galaxy candidates by comparing the number density of massive galaxies predicted by our SMPBH model with recent JWST result Eq. (1).

The expected number density of galaxies with $M_* > M_*^{\text{obs}}$, where M_*^{obs} represents the observational threshold of stellar mass, is given by (Boylan-Kolchin 2023)

$$n_{\text{gal}}(M_* \geq M_*^{\text{obs}}) = \int_{M_h^{\text{cut}}}^{\infty} \frac{dn(z^{\text{obs}}, M_h)}{dM_h} dM_h, \quad (27)$$

where $M_h^{\text{cut}} = M_h(M_*^{\text{obs}})$. Here, we speculate that each DM halo contains a single central galaxy, thus the relation between the halo and total stellar mass is $M_h(M_*) = M_*/(f_b \epsilon_*)$, where $f_b = \Omega_b/(\Omega_{\text{DM}} + \Omega_b) = 0.157$ is the baryon fraction and ϵ_* is the star formation efficiency. The comoving cumulative stellar mass density is

$$\rho(M_* \geq M_*^{\text{obs}}) = f_b \epsilon_* \int_{M_h^{\text{cut}}}^{\infty} M_h \frac{dn(z^{\text{obs}}, M_h)}{dM_h} dM_h. \quad (28)$$

The comoving cumulative stellar mass density ρ/ρ^{obs} with respect to (x_{cl}, ξ_0) is presented in Fig. 3, where ρ^{obs} is recent JWST observation Eq. (1). It can be seen that a population of clustering SMPBHs has a larger potential to reproduce the observation results. In contrast, we have $\log_{10}(\rho/\rho^{\text{obs}}) \simeq -1.41$ for Λ CDM model only and $\log_{10}(\rho/\rho^{\text{obs}}) \simeq -0.65$ for the same SMPBHs but with a Poisson distribution, i.e. the Λ CDM+PBH (Poisson) model, in the case of $\epsilon_* = 0.3$, both are not sufficient to explain JWST observation, while for a higher

$\epsilon_* = 0.7$, we also only have $\log_{10}(\rho/\rho^{\text{obs}}) \simeq -0.34$ and $\log_{10}(\rho/\rho^{\text{obs}}) \simeq 0.24$, respectively. Here, for the Λ CDM+PBH (clustering) model, we can naturally have $\log_{10}(\rho/\rho^{\text{obs}}) \sim 0$ for $\xi_0 = 10$, $x_{\text{cl}} \sim 1\text{Mpc}$ and $\epsilon_* \sim 0.3$.

In particular, there exists a parameter space that renders the model compatible with all constraints on clustering SMPBHs, see the gray shaded region and the purple line in Fig. 1. Taking into account these constraints, we observe that the enhancement of the comoving cumulative stellar mass density caused by the Λ CDM with clustering PBHs is about 2 times larger than that predicted by Poisson-distributed PBHs. This in certain sense reflects the advantage of initial clustering SMPBHs in explaining the high-redshift JWST massive galaxies.

5. DISCUSSION

High-redshift massive galaxies observed recently by JWST can be hardly reconcilable with the standard Λ CDM expectations. The existence of SMPBHs can enhance the matter power spectrum and thus the halo mass function, which helps to alleviate this conflict.

However, SMPBHs can cluster, see Huang & Piao (2023), and the merger of SMPBHs initially clustered might be the source of nano-Hertz gravitational wave background recently detected by PTA collaboration. This clustering not only sheds light on the origins of SMBHs but also accelerates the evolution of structures in the early universe. In this paper, we calculated the effect of the initial clustering SMPBHs on the matter power spectrum and the halo mass function, and found that compared with the Poisson-distributed SMPBHs model, the population of clustering SMPBHs

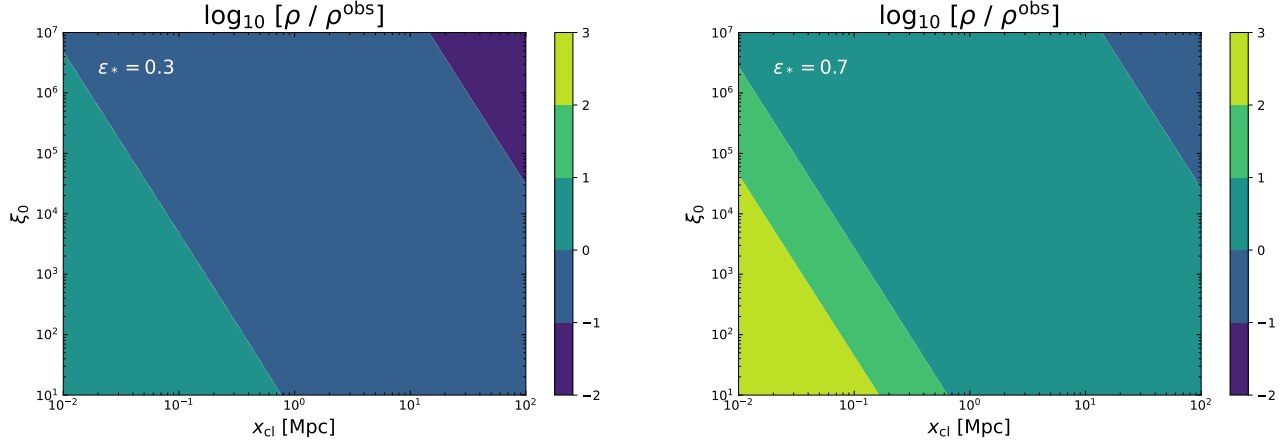


Figure 3. *Left panel:* The comoving cumulative stellar mass density at redshift $z^{\text{obs}} = 8$ as a function of (ξ_0, x_{cl}) , assuming a star formation efficiency $\epsilon_* = 0.3$. *Right panel:* Same as the left panel with a different star formation efficiency $\epsilon_* = 0.7$.

with $M_{\text{PBH}} \sim 10^9 M_{\odot}$ and $f_{\text{PBH}} \sim 10^{-3}$ can significantly accelerate the early formation of massive galaxies, and thus naturally explain recent JWST observation with a lower star formation efficiency. The collective results of our analysis is showed in Fig. 1.

The exploration of SMPBHs as potential progenitors of SMBHs that power high-redshift quasars presents intriguing insights into the evolution of our Universe. In this case the concept of initially clustered SMPBHs might be closely related to not only the evolution of our

primordial Universe but also the spatial distribution of massive objects and the birth of cosmic structures. The relevant issues are worth of further investigation.

- 1 We thank Hao-Yang Liu, Da-Shuang Ye for helpful
- 2 discussion. This work is supported by National Key
- 3 Research and Development Program of China (Grant
- 4 No. 2021YFC2203004), NSFC (Grant No.12075246),
- 5 and the Fundamental Research Funds for the Central
- 6 Universities.

REFERENCES

- Adil, S. A., Mukhopadhyay, U., Sen, A. A., & Vagnozzi, S. 2023, JCAP, 2023, 072
- Agazie, G., Anumalapudi, A., Archibald, A. M., et al. 2023, ApJL, 951, L8
- Arita, J., Kashikawa, N., Matsuoka, Y., et al. 2023, ApJ, 954, 210
- Bhowmick, A. K., Blecha, L., Torrey, P., et al. 2024, arXiv e-prints, arXiv:2406.14658
- Biagetti, M., Franciolini, G., & Riotto, A. 2023, ApJ, 944, 113
- Bogdán, Á., Goulding, A. D., Natarajan, P., et al. 2024, Nature Astronomy, 8, 126
- Boylan-Kolchin, M. 2023, Nature Astronomy, 7, 731
- Byrnes, C. T., Lesgourgues, J., & Sharma, D. 2024, arXiv e-prints, arXiv:2404.18475
- Cai, Y., Zhu, M., & Piao, Y.-S. 2024, PhRvL, 133, 021001
- Carr, B., Kohri, K., Sendouda, Y., & Yokoyama, J. 2021, Reports on Progress in Physics, 84, 116902
- Carr, B., & Silk, J. 2018, MNRAS, 478, 3756
- Carr, B. J., Clesse, S., García-Bellido, J., Hawkins, M. R. S., & Kühnel, F. 2024, PhR, 1054, 1
- Colazo, P. E., Stasyszyn, F., & Padilla, N. 2024, A&A, 685, L8
- Cole, S., & Kaiser, N. 1989, MNRAS, 237, 1127
- Croom, S. M., Smith, R. J., Boyle, B. J., et al. 2004, MNRAS, 349, 1397
- Davari, Z., Ashoorioon, A., & Rezazadeh, K. 2023, arXiv e-prints, arXiv:2311.15083
- De Luca, V., Franciolini, G., & Riotto, A. 2023, PhRvL, 130, 171401
- De Luca, V., Franciolini, G., Riotto, A., & Veermäe, H. 2022, PhRvL, 129, 191302
- Depta, P. F., Schmidt-Hoberg, K., Schwaller, P., & Tasillo, C. 2023, arXiv e-prints, arXiv:2306.17836
- Desjacques, V., & Riotto, A. 2018, PhRvD, 98, 123533
- Ding, Q., Nakama, T., Silk, J., & Wang, Y. 2019, PhRvD, 100, 103003
- Efstathiou, G., & Rees, M. J. 1988, MNRAS, 230, 5p
- EPTA Collaboration, InPTA Collaboration, Antoniadis, J., et al. 2023, A&A, 678, A50
- Escrivà, A., Kühnel, F., & Tada, Y. 2022, arXiv e-prints, arXiv:2211.05767

- Forconi, M., Giarè, W., Mena, O., et al. 2024, *JCAP*, 2024, 097
- Franciolini, G., Kehagias, A., Matarrese, S., & Riotto, A. 2018, *JCAP*, 2018, 016
- Furtak, L. J., Labbé, I., Zitrin, A., et al. 2023, arXiv e-prints, arXiv:2308.05735
- Goulding, A. D., Greene, J. E., Setton, D. J., et al. 2023, *ApJL*, 955, L24
- Gouttenoire, Y., Trifinopoulos, S., Valogiannis, G., & Vanvlasselaer, M. 2023, arXiv e-prints, arXiv:2307.01457
- Gow, A. D., Assadullahi, H., Jackson, J. H. P., et al. 2023, *EPL (Europhysics Letters)*, 142, 49001
- Green, A. M. 2024, *Nuclear Physics B*, 1003, 116494
- Green, A. M., & Kavanagh, B. J. 2021, *Journal of Physics G Nuclear Physics*, 48, 043001
- Greene, J. E., Labbe, I., Goulding, A. D., et al. 2024, *ApJ*, 964, 39
- Harikane, Y., Zhang, Y., Nakajima, K., et al. 2023, *ApJ*, 959, 39
- Hooper, D., Ireland, A., Krnjaic, G., & Stebbins, A. 2024, *JCAP*, 2024, 021
- Huang, H.-L., Cai, Y., Jiang, J.-Q., Zhang, J., & Piao, Y.-S. 2023, arXiv e-prints, arXiv:2306.17577
- Huang, H.-L., Jiang, J.-Q., & Piao, Y.-S. 2024, *PhRvD*, 109, 063515
- Huang, H.-L., & Piao, Y.-S. 2023, arXiv e-prints, arXiv:2312.11982
- Hütsi, G., Raidal, M., Urrutia, J., Vaskonen, V., & Veermäe, H. 2023, *PhRvD*, 107, 043502
- Inman, D., & Ali-Haïmoud, Y. 2019, *PhRvD*, 100, 083528
- Iocco, F., & Visinelli, L. 2024a, *Physics of the Dark Universe*, 44, 101496
- . 2024b, arXiv e-prints, arXiv:2403.13068
- Jiao, H., Brandenberger, R., & Refregier, A. 2023, *PhRvD*, 108, 043510
- Kasai, K., Kawasaki, M., Kitajima, N., et al. 2023, *JCAP*, 2023, 049
- Kasai, K., Kawasaki, M., Murai, K., & Neda, S. 2024, arXiv e-prints, arXiv:2405.09790
- Kawasaki, M., Murai, K., & Nakatsuka, H. 2021, *JCAP*, 2021, 025
- Kokorev, V., Fujimoto, S., Labbe, I., et al. 2023, *ApJL*, 957, L7
- Kovács, O. E., Bogdán, Á., Natarajan, P., et al. 2024, *ApJL*, 965, L21
- Labbé, I., van Dokkum, P., Nelson, E., et al. 2023, *Nature*, 616, 266
- Larson, R. L., Finkelstein, S. L., Kocevski, D. D., et al. 2023, *ApJL*, 953, L29
- Li, H.-H., Ye, G., & Piao, Y.-S. 2021, *Physics Letters B*, 816, 136211
- Li, M., & Wang, Y. 2009, *JCAP*, 2009, 033
- Li, S., Liu, Y., & Piao, Y.-S. 2009, *PhRvD*, 80, 123535
- Liu, B., & Bromm, V. 2022, *ApJL*, 937, L30
- . 2023, arXiv e-prints, arXiv:2312.04085
- Madau, P., & Rees, M. J. 2001, *ApJL*, 551, L27
- Maiolino, R., Scholtz, J., Curtis-Lake, E., et al. 2023a, arXiv e-prints, arXiv:2308.01230
- Maiolino, R., Scholtz, J., Witstok, J., et al. 2023b, arXiv e-prints, arXiv:2305.12492
- Matthee, J., Naidu, R. P., Brammer, G., et al. 2023, arXiv e-prints, arXiv:2306.05448
- Menci, N., Adil, S. A., Mukhopadhyay, U., Sen, A. A., & Vagnozzi, S. 2024, arXiv e-prints, arXiv:2401.12659
- Nakama, T., Carr, B., & Silk, J. 2018, *PhRvD*, 97, 043525
- Natarajan, P., Pacucci, F., Ricarte, A., et al. 2024, *ApJL*, 960, L1
- Padmanabhan, H., & Loeb, A. 2023, *ApJL*, 953, L4
- Parashari, P., & Laha, R. 2023, *MNRAS*, 526, L63
- Paraskevas, E. A., çam, A., Perivolaropoulos, L., & Akarsu, Ö. 2024, *PhRvD*, 109, 103522
- Pizzati, E., Hennawi, J. F., Schaye, J., & Schaller, M. 2024a, *MNRAS*, 528, 4466
- Pizzati, E., Hennawi, J. F., Schaye, J., et al. 2024b, arXiv e-prints, arXiv:2403.12140
- Planck Collaboration, Akrami, Y., Arroja, F., et al. 2020, *A&A*, 641, A10
- Press, W. H., & Schechter, P. 1974, *ApJ*, 187, 425
- Reardon, D. J., Zic, A., Shannon, R. M., et al. 2023, *ApJL*, 951, L6
- Sasaki, M., Suyama, T., Tanaka, T., & Yokoyama, S. 2018, *Classical and Quantum Gravity*, 35, 063001
- Schneider, A., Giri, S. K., & Mirocha, J. 2021, *PhRvD*, 103, 083025
- Sharma, D., Lesgourgues, J., & Byrnes, C. T. 2024, arXiv e-prints, arXiv:2404.18474
- Sheth, R. K., Mo, H. J., & Tormen, G. 2001, *MNRAS*, 323, 1
- Sheth, R. K., & Tormen, G. 1999, *MNRAS*, 308, 119
- Suyama, T., & Yokoyama, S. 2019, *Progress of Theoretical and Experimental Physics*, 2019, 103E02
- Tada, Y., & Yokoyama, S. 2015, *PhRvD*, 91, 123534
- Übler, H., Maiolino, R., Curtis-Lake, E., et al. 2023a, *A&A*, 677, A145
- Übler, H., Maiolino, R., Pérez-González, P. G., et al. 2023b, arXiv e-prints, arXiv:2312.03589
- Ünal, C., Kovetz, E. D., & Patil, S. P. 2021, *PhRvD*, 103, 063519

Xu, H., Chen, S., Guo, Y., et al. 2023, *Research in Astronomy and Astrophysics*, 23, 075024

York, D. G., Adelman, J., Anderson, John E., J., et al. 2000, *AJ*, 120, 1579

Young, S., & Byrnes, C. T. 2015, *JCAP*, 2015, 034

Yuan, G.-W., Lei, L., Wang, Y.-Z., et al. 2023, arXiv e-prints, arXiv:2303.09391

Zhang, S., Bromm, V., & Liu, B. 2024, arXiv e-prints, arXiv:2405.11381